

# Flux-Switching Permanent Magnet Machine Drive System for Plug-in Hybrid Electrical Vehicle

Wei Xu, Jianguo Zhu, Yongchang Zhang, Yi Wang, Yongjian Li, Jiefeng Hu

School of Electrical, Mechanical and Mechatronic Systems, University of Technology, Sydney, NSW, Australia

E-mail: weixuhappy@ieee.org; joe@eng.uts.edu.au

**Abstract**—Plug-in hybrid electric vehicle (PHEV) depends mostly on the electric drive system where the internal combustion engine just acts as the auxiliary unit, which has strict constraints for the drive machine. According to the Toyota Prius configuration, one novel PHEV drive system in this paper has been brought forward which primarily includes one drive machine operating as both motor and generator, energy storage unit combining supercapacitor and battery. In the novel PHEV, the ideal tendency is to use the drive machine over the entire torque/speed range, including starting/acceleration, high speed cruising, regenerative braking, etc. The flux-switching permanent magnet machine (FSPMM) for the drive system has been studied in details. Firstly, the structure and operation principle are analyzed theoretically. In order to achieve higher torque/power density and lower torque ripple, FSPMM with 6/7 (stator/rotor) poles and 12/14 poles according to plenty of investigations are optimized based on our setting objective function decided by actual projects. Moreover, it analyzes several typical performance curves, such as cogging/rating torque, flux linkage, back-EMF, and self-/mutual- inductances. Finally the flux-weakening ability and efficiency are estimated by experience. The results indicate that FSPMM is one ideal candidate for our PHEV drive system for its strong thermal dissipation ability, good mechanical robustness, strong flux-weakening ability, etc.

**Keywords**-*Plug-in hybrid electric vehicle (PHEV); flux-switching permanent magnet machine (FSPMM); flux-weakening ability; thermal dissipation; mechanical robustness.*

## I. INTRODUCTION

Most vehicles running on roads today are propelled by internal combustion engines (ICEs). Despite their wide diffusion and the remarkable evolution during the last century, ICEs have been afflicted by many defects, notably their low energy efficiency traditionally no more than 30%, carbon dioxide emission, and dependence on crude oil. According to the investigation released by the USA environmental protection agency (EPA), conventional ICE vehicles currently contribute 40-50% of ozone, 80-90% of carbon monoxide, and 50-60% of air toxins found in urban areas. Fig.1 indicates total CO<sub>2</sub> emission proportion in China by field. Fig.2 shows global vehicle CO<sub>2</sub> emission proportion by region, North America, the greatest one, is more than one third, followed by China close to one fifth, and the third is European region.

However, the amount of crude oil in the world is limited, which will be used up sooner or later. According to statistics of American DOE, gasoline price has been increased 2 times during the past 8 years, which is indicator of growing tension between supply and demand. Furthermore, the emission of green house gases emitted by cars has already made the world

weather warmer which affects human being's normal living. Therefore, the increase of fuel economy is very important for actual automobile development so as to decrease its dependence on oil, and reduce carbon dioxide emission.

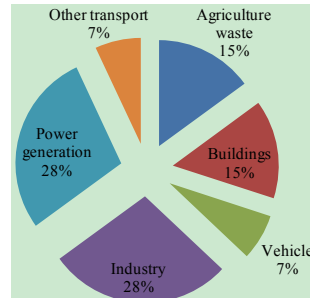


Fig.1. Total CO<sub>2</sub> emission proportion in China by field.

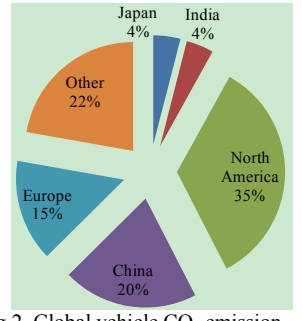


Fig.2. Global vehicle CO<sub>2</sub> emission proportion by region.

Battery powered electrical vehicle (EV) can bring some merits over the ICE cars, such as reduced environmental pollution and high energy efficiency. However, its operation range is far less competitive than ICE vehicles because of the low battery power density. HEVs have advantages of both EV and ICE cars, which employ two power sources, a primary unit ICE fuelled by a petrol tank and a supplementary unit of motor and generator fuelled by a battery and/or super capacitor bank. An early version of HEVs, also known as the micro HEV, is implemented on the basis of the conventional ICE powered vehicles by increasing the power capacity of the starter generator, which functions as the starter for ICE when the vehicle is started and a regenerative brake when the vehicle reduces its speed. Because of various electrical and mechanical constraints, the function of regenerative braking is possible but not very effective. A modern HEV is propelled jointly by the ICE and the electrical motor. In the current commercial versions, the ICE plays the major propulsion, while the electrical motor functions only as the supplementary drive when there is a need for extra torque, and the regenerative braking is realized by a separate generator.

By the great development of battery technology and power electronics, plug-in hybrid electrical vehicle (PHEV) has been paid much more attention both by academia and industry. Different with HEV, drive machine in the PHEV plays the primary role while the ICE just acts as the auxiliary unit which only works in the initial starting, acceleration, hill-climbing, and other urgent cases. In theory, the PHEV could bring zero carbon dioxide emission if charged by green sources such as wind, solar, methane (from landfills), hydro, and diesels powered from synthetic fuel, which are some of the green

generation being interconnected with the utility at the distribution level.

Fig.3 is one novel PHEV drive system configuration presented in [1, 2]. Different with the typical HEV structure in Toyota Prius illustrated in Fig.4, the novel configuration has the following traits. (1) Strong energy storage unit combining battery with high energy density and supercapacitor with high power density. The battery and supercapacitor getting the electricity from the grid by the charger supply the energy to drive the electrical machine, or store the regenerative energy during braking so as save amount of energy. (2) Only one drive machine acts as motor or generator in different working styles. For the sole drive machine, the connection between mechanical and electrical ports is much simple. Furthermore, the drive machine has more compact volume, higher efficiency for its lower copper and iron losses. (3) Flexible energy management strategies. There are four typical states in our novel PHEV structures, including the energy from storage unit to drive machine, kinetic energy from drive machine to storage unit, energy from ICE to storage unit, and energy from ICE to drive machine, *etc.* [2]. It is also flexible to control the drive machine by the help of energy management strategy provided in [2].

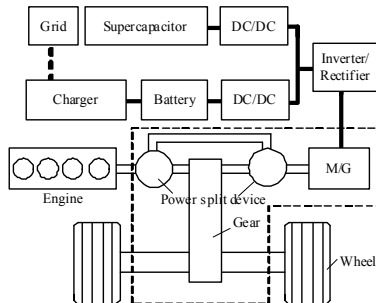


Fig.3. Provided PHEV system configuration.

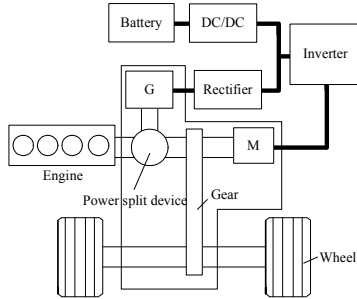


Fig.4. Toyota hybrid system configuration.

However, the novel PHEV configuration brings more strict constraints for the drive machine in addition to some traditional requirements, particularly in the aspects of heat dissipation ability, structure robustness, flux-weakening ability, and working redundancy capability. To the authors' best knowledge, four kinds of ordinary machines, involving DC machine, switched reluctance machine (SRM), induction machine, and permanent magnet synchronous machine (PMSM) with PM placed in rotor, could not be satisfied with the aforementioned four special aspects simultaneously.

One emerging flux-switching permanent magnet machine (FSPMM) combining the SRM with simple rotor structure

capable of reaching extremely high speed and PMSM with higher torque/power density will be discussed in this paper. It is organized as follows. In Section II, the typical topology and operation principle of FSPMM are briefly introduced. The electromagnetic optimal design of FSPMM is given out in Section III. In Section IV, it makes the main performance analysis of FSPMM. Final conclusions are drawn in Section V.

## II. STRUCTURE AND OPERATION PRINCIPLE

Fig.5 gives out brief introduction on the FSPMM with 12/10 poles, including the whole structure, PM arrangement, and PM flux linkage road line [4]. It can be found from Fig.5 (a) that the rotor of the machine is similar to that of a SRM. Compared to SRM, the main difference lies in the configuration of magnets in the stator, containing 12 segments of "U"-shape magnetic cores, between which 12 pieces of magnets are insert pre-magnetized circumferentially in alternative opposite directions. Dislike the traditional PMSM with PMs in the rotor, the placement of both magnets and windings in the stator is easy to be cooled for its large space or surface, which is greatly attractive to the aerospace and EV applications where the ambient temperature of the machine are comparatively higher for compact volume. The FSPM machine with concentrated windings on each pole is wound around the two adjacent teeth with a piece of magnet in the middle, which leads to low copper consumption due to short end-windings. Moreover, it employs the feature of independent electric and magnetic circuits among phases so to offer the possibility of independent control and operation among phases [5].

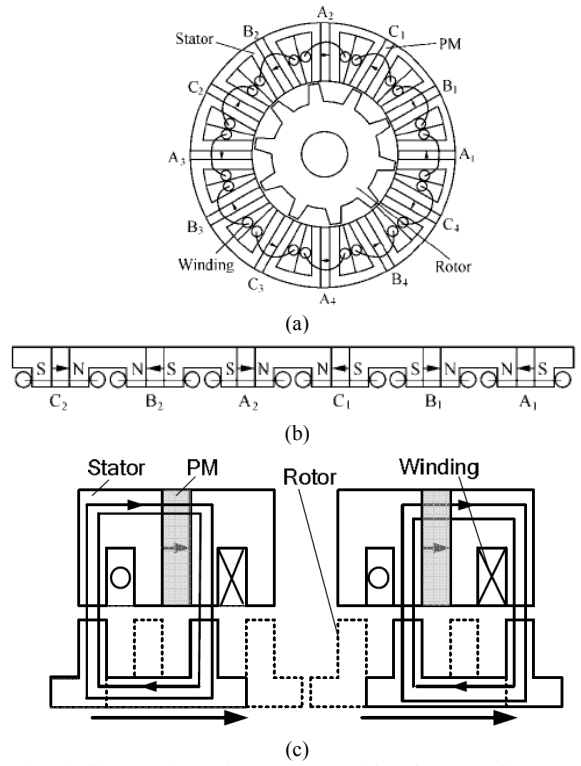


Fig.5. Simple diagram of a 3-phase FSPMM with 12/10 (stator/rotor) poles [4].  
(a) The whole structure. (b) PM placement. (c) Flux linkage.

The PM configuration is shown in Fig.5 (b). In simplification, only half of the stator due to symmetry is

discussed here [4]. At the position shown in Fig. 5(a), the phase A PM flux linkage gets to the maximum. The polarity of flux in coils A1 and coil A2 is identical with slight difference in their amplitudes due to magnetic circuit differences and partly saturation. The relative position between the PMs and coils can be described as: A1+ N\_B1- S\_C1- N\_A2+ S\_B2- N\_C2- where N/S denotes the polarity of magnets and +/-denotes the opposite polarity of stator coils. When the rotor rotates 18 mechanical degrees anticlockwise from the position in Fig.5 (a), both fluxes of coils A1 and A2 will change from positive to negative simultaneously while the amount of flux is unchanged.

The two pictures in Fig.5 (c) indicate that the PM flux linkage path changes with different rotor positions. It seems that one switching placed in the stator pole to be turned on or off to control the PM flux linkage through the stator left or right side. Different with those of double salient permanent magnet machine and SRM, the FSPMM has bipolar flux linkage curve, which could be excited by bipolar current so as to have higher average torque. In addition, it has shorter magnetic circuit that may result in low iron loss in the stator back-iron and lower leakage inductance. The operation principle of FSPM machine can be described in Fig.6 [6].

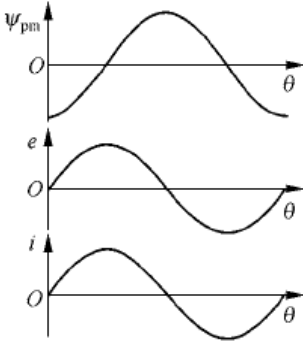


Fig.6. Operation principle of FSPMM.

### III. ELECTROMAGNETIC DESIGN

There are a lot of feasible combinations of stator and rotor pole numbers in FSPMM given by

$$\begin{cases} N_s = k_1 m \\ N_r = N_s \pm k_2 \end{cases} \quad (k_1, k_2 = 1, 2, 3, \dots) \quad (1)$$

where  $N_s/N_r$  is the number of stator/rotor pole,  $m$  is the number of phases,  $k_1$  is an integer number when  $m$  is an even number, but  $k_1$  should be an even number when  $m$  is an odd number since the number of stator poles must be even. In order to quantitatively compare the torque or power of various structures, we set the precondition: outer radius is 80mm, lamination depth 60 mm, and the split ratio (inner rotor radius to outer radius) 0.6 based on plenty of practice. The torque curves of stator with 6 and 12 in three phases are illustrated in Fig.7, and self-inductance curves in Fig.8. For the double salience occurring in both stator and rotor, there exists torque ripple in different rotor position for the changing equivalent air gap lengths. The torque ripple ratio  $K_T$  is defined by

$$K_T = \sqrt{\frac{1}{T} \int_0^T (T - T_{\text{avg}})^2 dt} / T_{\text{avg}} \quad (2)$$

where  $T_{\text{avg}}$  is the average torque.  $K_T$  is one ratio to describe torque ripple RMS value, which takes the ripple in different rotor position into consideration.

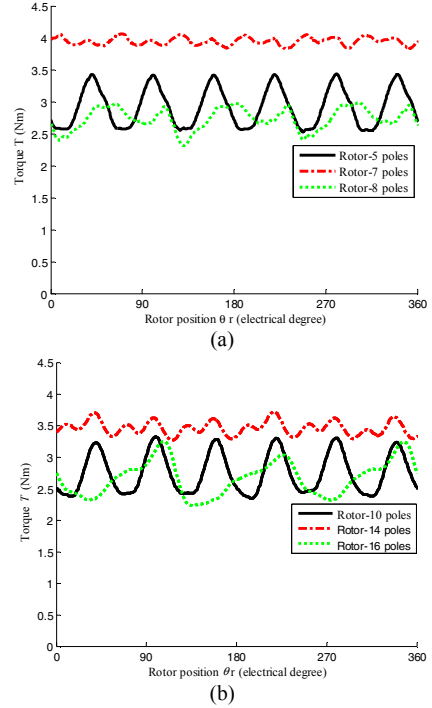


Fig.7. Torque versus rotor position. (a) 6-pole stators. (b) 12-pole stators.

The average torque and torque ripple are summarized in Table I. It is evident that FSPMM with 6/7 and 12/14 poles have the highest average torque and lowest torque ripple among 6 different structures, which are hence chosen as our backups for the novel drive system.

TABLE I  
TORQUE AND TORQUE RIPPLE OF DIFFERENT FSPMMs

| Items               | 6/5   | 6/7  | 6/8  | 12/10 | 12/14 | 12/16 |
|---------------------|-------|------|------|-------|-------|-------|
| Average torque (Nm) | 2.92  | 3.95 | 2.73 | 2.75  | 3.45  | 2.67  |
| Torque ripple (%)   | 10.36 | 1.49 | 6.34 | 11.51 | 3.10  | 10.42 |

It is noted that there are great magnetic saturation existing in the FSPMM, particularly in the fringe of stator pole, edge of PM, teeth of the rotor, and so on. The flux linkage nephograms are indicated in the Fig.8, where the maximal could reach more than 2.5 Tesla. Fig.9 shows the air gap flux density distribution versus rotor position. Different with those of traditional PM machines, the flux density is not ideally sinusoidal. It has higher value in the adjacent domain of stator teeth or rotor pole. In order to improve the performance indexes, such as torque/power density, efficiency, torque ripple, and reduce the partial magnetic saturation, it is very necessary to optimize the structure parameters. By plenty of investigation on the electromagnetic design, some key structure sizes for the FSPMM, involving the width of stator pole, PM thickness, width of rotor pole, series number of winding in each pole, etc., could be optimized by the objective function defined as,

$$\text{Max } f = a_1 \frac{T - T_w}{T_b - T_w} + a_2 \frac{\eta - \eta_w}{\eta_b - \eta_w} + a_3 \frac{K_T - K_{Tw}}{K_{Tb} - K_{Tw}} \quad (3)$$

where  $T$  is the optimal torque,  $T_w$  the worst torque,  $T_b$  the best torque,  $\eta$  the optimal efficiency,  $\eta_w$  the worst efficiency,  $\eta_b$  the best efficiency,  $K_{Tw}$  the worst torque ripple ratio, and  $K_{Tb}$  the best torque ripple ratio;  $a_1$ ,  $a_2$ ,  $a_3$  are weighting ratios for different optimal variables [5]. The objective function is one normalized value, where  $a_1$ ,  $a_2$ ,  $a_3$ ,  $T_w$ ,  $T_b$ ,  $\eta_w$ ,  $\eta_b$ ,  $K_{Tw}$ ,  $K_{Tb}$  should be decided dependent of actual project requirements. The optimal electromagnetic design flow chart is shown in Fig.10. The final dimensions should be decided by many iterations constrained by the objective function to finally agree with the performance requirements.

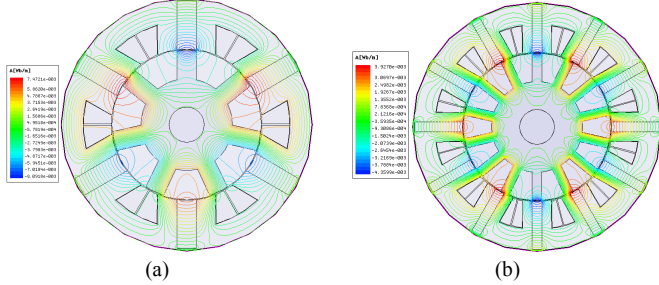


Fig.8. Flux linkage nephogram. (a) 6/7 poles. (b) 12/14 poles.

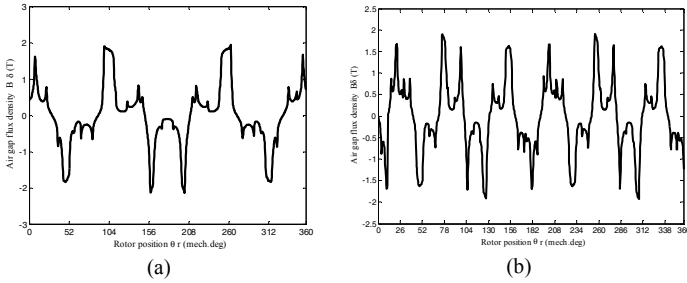


Fig.9. Air gap flux density distribution versus rotor position.  
(a) 6/7 poles. (b) 12/14 poles.

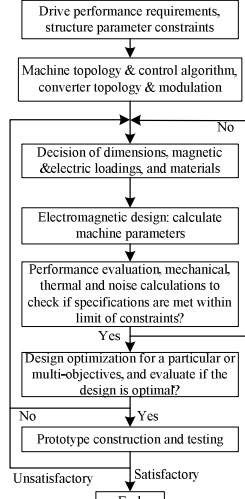


Fig.10. Optimal electromagnetic design procedure.

#### IV. PERFORMANCE ANALYSIS

According to the full investigation of our provided PHEV executed by PSAT, one famous automobile simulation software, from the system view, the rated power of the drive machine is approximately 75kW@3000rpm [5]. In order to

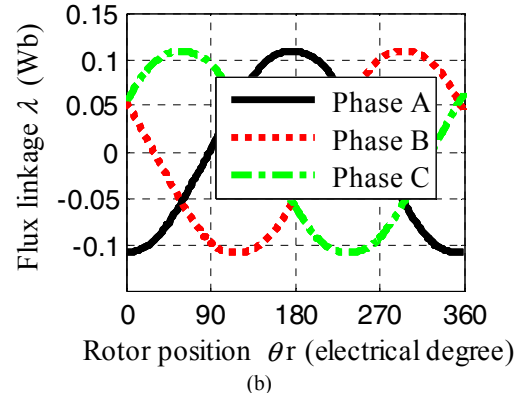
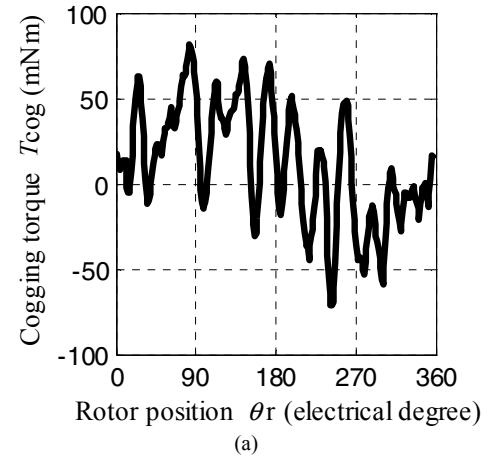
save the cost and verify the theoretic analysis, two prototypes including 6/7 and 12/14 poles are optimized whose dimensions are given in the Table II. The two machines have the same outer radius with 40.6 mm, and split ratio with 0.613 (the rotor out radius to the stator out radius).

TABLE II  
MAIN DIMENSIONS OF TWO MACHINES (Length unit: mm)

| Items          | FSPM (6/7)              | FSPM (12/14) |
|----------------|-------------------------|--------------|
| Stator         | Outer radius            | 40.6         |
|                | York height             | 4.5          |
|                | Pole width              | 15.2         |
|                | Pole height             | 9.8          |
|                | Winding number per pole | 100          |
|                | Width                   | 3.9          |
| PM             | Height                  | 13.8         |
|                | Air gap length          | 0.5          |
|                | Pole width              | 7.8          |
| Rotor          | Pole height             | 6            |
|                | York                    | 7.4          |
|                | Radius of shaft         | 6.8          |
| Depth of model |                         |              |
|                |                         |              |

#### A. Typical Performance Curves

Typical performance curves of FSPMM with 6/7 poles include the cogging torque, flux linkage in no load, excited rating phase current, back-EMF in no load, and rating torque@3000 rpm, are illustrated in Fig.11.



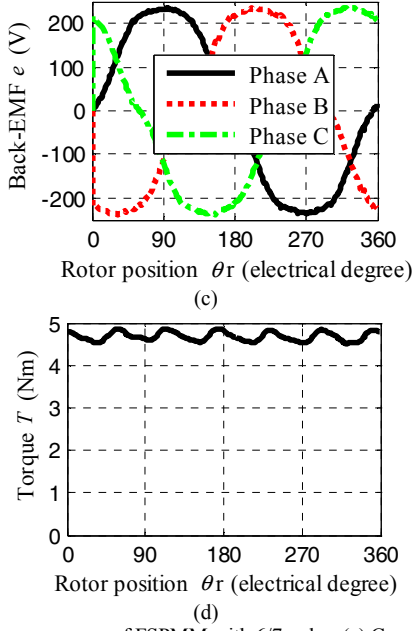


Fig.11. Performance curves of FSPMM with 6/7 poles. (a) Cogging torque. (b) Flux linkage. (c) Back-EMF. (d) Rated torque @3000 rpm.

Similarly, typical performance curves of FSPMM with 12/14 poles are given out in Fig.12. As shown in Figs.11 and 12, the cogging torque is only relative with structure parameters, especially the widths of stator and rotor poles, slot depth, PM thickness, etc. For the double salient trait, the cogging torque cannot be eliminated, which could be decreased by optimizing the structures and adopting rotor skewing techniques. For the almost half PM thickness in FSPMM with 12/14 compared with those of 6/7, it also has about half amplitude of phase flux linkage. The back-EMF waves seem sinusoidal with bipolarity, and hence the FSPMMs could be excited by BLAC operation principle.

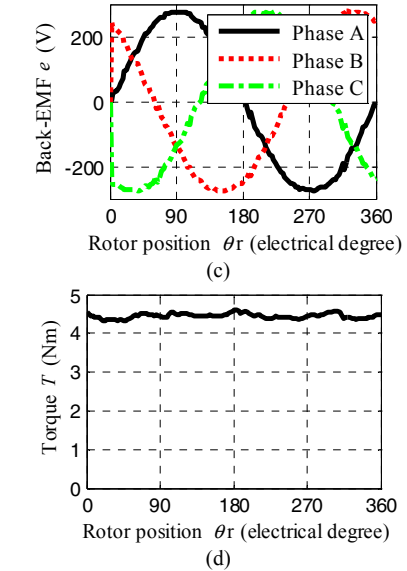
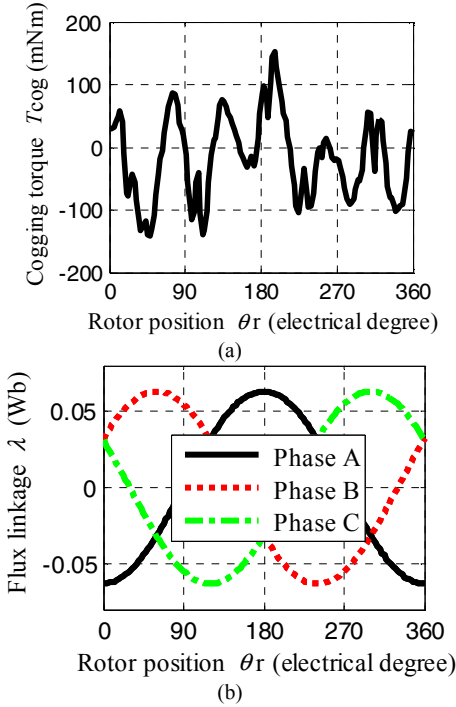


Fig.12. Performance curves of FSPMM with 12/14 poles. (a) Cogging torque. (b) Flux linkage. (c) Back-EMF. (d) Rated torque @3000 rpm.

### B. Self- and Mutual- Inductances

The average torque and torque ripple are summarized in the Table III. For larger leakage inductance in FSPMM with 12/14 poles, it has lower average torque than that of 6/7 poles. Fortunately, it has lower torque ripple for more symmetry magnetic path. The self- and mutual- inductances are functions versus rotor position. Strictly speaking, they are also affected by the excited current for nonlinear saturation. Fig.13 is the inductance diagrams in the rating current. For twice number of the stator poles, FSPMM with 12/14 has almost half self- and mutual inductance as those of 6/7.

| TABLE III<br>AVERAGE TORQUE AND TORQUE RIPPLE |      |       |
|---|------|-------|
| Items   | 6/7  | 12/14 |
| Average torque (Nm)                           | 4.68 | 4.45  |
| Torque ripple (%)                             | 2.27 | 1.43  |

### C. Flux-Weakening Ability

According to the definition in [4], the flux-weakening ability can be expressed by

$$\beta = \frac{\Psi_m}{\Psi_m - \Psi_d} = \frac{\Psi_m}{\Psi_m - L_d i_d} \quad \beta = \frac{\Psi_m}{\Psi_m - \Psi_d} = \frac{\Psi_m}{\Psi_m - L_d i_d} \quad (4)$$

where \$\Psi\_m\$ is permanent magnet flux linkage, \$L\_d\$ the equivalent \$d\$-axis inductance, \$i\_d\$ the \$d\$-axis current. This index is very important to PHEV application that affects the high speed cruising range. By adjusting the structure parameters, \$L\_d\$ could become larger than \$q\$-axis inductance \$L\_q\$, but the torque ripple might become much serious. Hence, one compromise value between \$\beta\$ and torque ripple could be chosen, which are shown in Table IV. For comparatively lower PM flux linkage and larger leakage inductance, FSPMM with 12/14 has stronger flux weakening ability.

| TABLE IV<br>FLUX-WEAKENING ABILITY |      |       |
|------------------------------------|------|-------|
| Items                              | 6/7  | 12/14 |
| Flux weakening ability             | 4.32 | 5.08  |

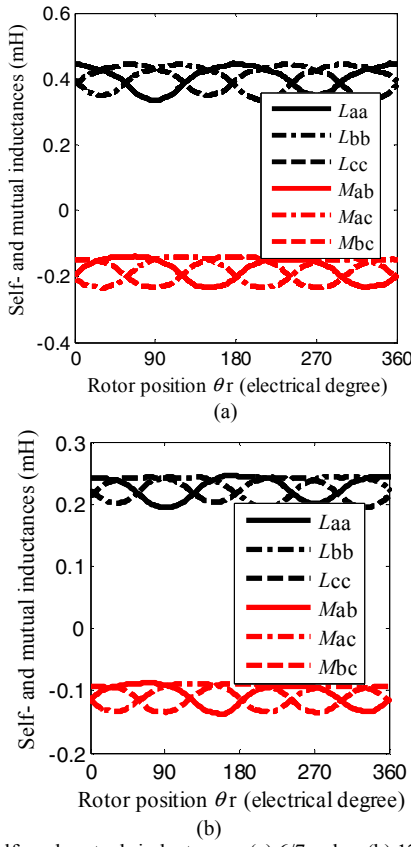


Fig.13. Self- and mutual- inductances. (a) 6/7 poles. (b) 12/14 poles.

#### D. Efficiency

The power loss mainly includes armature winding (copper) loss, iron loss, friction and stray loss. It is very easy to calculate the copper loss, and the friction and stray loss could be estimated by experience. The iron loss calculation is given below. Based on the data provided by the manufacturer, the iron losses  $P_t$  under time-varying flux is separated into a hysteresis loss component  $P_h$  and eddy current component  $P_c$ , both in watts per kilogram as indicated below.

$$P_t = P_h + P_c = k_h f^2 B_m^\alpha + k_e f^2 B_m^\alpha \quad (5)$$

where  $f$  and  $B$  are the frequency and the peak value of the magnetic flux density, respectively;  $k_h$ ,  $k_e$  and  $\alpha$  are the loss coefficients of one novel material, M19\_29G. The three coefficients could be calculated automatically by commercial finite element algorithm software, such as ANSYS, after entering the B-H data of the silicon steel. The efficiency is estimated in Table V. For lower torque and larger stator resistance, FSPMM with 12/14 has lower efficiency than that of 6/7.

TABLE V  
EFFICIENCY ESTIMATION

| Items          | 6/7  | 12/14 |
|----------------|------|-------|
| Efficiency (%) | 92.4 | 90.5  |

#### V. CONCLUSIONS

PHEVs have been paid much attention recently for their less or even zero emission to our atmosphere for their propulsions by the electricity. Hence, the electric drive system

as one of the most important units plays the key role in the final PHEV successful commercialization. In order to reduce the volume and complexity of mechanical construction, increase the efficiency, etc., one novel PHEV configuration with only one machine as motor or generator, and energy storage unit combining both supercapacitor and battery has been provided. For continuous working state, the drive machine should have strong thermal dissipation ability, good robustness, and redundancy capability even in some serious conditions except for the traditional requirements for the hybrid electrical vehicle.

This paper firstly analyzes the primary traits of FSPMM, one emerging stator-PM machine, including the mechanical structure, operation principle, fundamental performance curves. For the double salient structure, the FSPMM has torque ripple and partial magnetic saturation. Then it discusses how to optimize the FSPMM based on the objective function according to the project requirement. Finally, the optimal schemes are given out as well as comprehensive analysis of typical performance curves, involving cogging torque, flux-linkage, back-EMF, rating torque, self- and mutual-inductances, flux-weakening ability, efficiency, etc.

Some important features of FSPMM are summarized here. (1) FSPMMs have bipolar flux linkages for its special magnetic circuits, which could make full use of the PMs. They have higher torque/power densities than those of traditional PM machines. (2) They have higher efficiency for shorter concentrating end-windings and more compact volume. (3) Due to larger  $d$ -axis inductances, FSPMMs have larger flux-weakening ability without extra DC excitation coils. For larger surface area with stator iron, PMs could not be demagnetized in the continuous operation at the rating point. (4) Due to the sinusoidal flux linkage and EMF waves, FSPMM could be operated completely in the BLAC model by skewing rotor. The control schemes of AC machines can be adopted in the FSPMMs directly.

The fundamental investigations indicate that FSPMM is one good candidate for our novel PHEV drive system for its good thermal dissipation capability, strong robustness suitable for high speed application, good flux-weakening ability more than four times, high torque/power density from the bipolarity of phase flux linkage.

#### REFERENCES

- [1] W. Xu, etc., "Drive system analysis of a novel plug-in hybrid vehicle", in *Proc. IEEE Industrial Electronics Society*, 2009, pp.3717-3722.
- [2] S.A. Rahman, N. Zhang, and J.G. Zhu, "Modelling and simulation of an energy management system for plug-in hybrid electric vehicles", in *Proc. Australasian University Power Engineering Conf.*, 2008, pp.1-6.
- [3] H. Oba, "Characteristics and analysis of efficiency of various hybrid systems," *Report of Toyota Motor Corporation*, 2004, pp.935-957.
- [4] W. Hua, "Inductance characteristics of 3-phase flux-switching permanent magnet machine with doubly-salient structure," *Transactions of China Electrotechnical Society*, vol.22, no.11, pp. 25-32, Nov. 2007.
- [5] W. Xu, etc., "Characterization of advanced drive system for hybrid electric vehicles," in *Proc. IEEE Int. Conf. Electrical Machines and Systems*, 2010, in press.
- [6] W. Hua, M. Cheng, etc., "Analysis and optimization of back EMF waveform of a flux-switching permanent magnet motor." *IEEE Trans. Energy Convers.*, vol. 23, no.3, pp. 727-733, Sept. 2008.
- [7] Ansoft company, *Study of a permanent magnet motor with MAXWELL 2D: example of the 2004 Prius IPM motor*, Sept. 2008.

# AUPEC 2010

**20th Australasian Universities Power Engineering Conference**

*“Power Quality for the 21<sup>st</sup> Century”*



**5 – 8 December 2010**

**University of Canterbury, Christchurch, New Zealand**

## **WELCOME TO AUPEC 2010**

On behalf of the Organising Committee for the Australasian Universities Power Engineering Conference 2010 I welcome you to Christchurch, New Zealand.

This is the second opportunity we have had to host AUPEC and only the second time the conference has been held outside of Australia. Over the intervening seven years since the University of Canterbury first hosted AUPEC in 2003 it has truly become an Australasian affair. With each annual AUPEC conference we are experiencing a wider international participation, particularly from those countries geographically close to Australia and New Zealand.

The first electrical engineering degree programmes in New Zealand were offered at the University of Canterbury in 1901 and electric power engineering tertiary education at the University of Canterbury continues to have a strong presence today. Our major sponsors from within the University are the College of Engineering, the Department of Electrical and Computer Engineering and principal sponsoring host, the Electric Power Engineering Centre (EPECentre), which is New Zealand's Centre of excellence for electric power engineering.

This year the committee received 212 abstracts from as far afield as Malaysia and Iran. A total of 154 papers were received for the final review and 129 have been accepted for presentation in four parallel sessions over three days.

I wish to acknowledge the significant financial support offered by the Australian Power Institute. The level of financial support we have received from our industry partners has also been gratifying. Thank you to all of those sponsors, through your generosity we have been able to put together an exciting programme of events at a reasonable cost to the participants.

Christchurch is known as the Garden City and I am sure you will agree that it is a beautiful city. Unfortunately as you travel around the city you will notice various battle scars from wrangling earthquakes, but by and large Christchurch has got back to normality quite quickly. Inland from Christchurch lies the Canterbury Plains and the Southern Alps, while adjacent to the city is the French township of Akaroa on Banks Peninsula. Whether you are confined to the city during your stay or have the opportunity to travel more widely, I hope that you can make time to see some of New Zealand's fabulous scenery.

Richard Duke  
General Chair AUPEC2010

|           |   |   |   |   |  |
|-----------|---|---|---|---|--|
| 0930-0935 | E1 INTRO DAY III - Joseph Lawrence, EPECentre, University of Canterbury   |   |   |   |  |
|           | <b>SPECIAL PRESENTATION</b> "The World's Coolest Windfarm in Antarctica"<br>Ray Brown, Transmission Development Manager and Craig Brown, Transmission Specialist, Meridian Energy   |   |   |   |  |
| 0935-1005 | E1  | E11   | E14   | E16   |  |
|           | <b>SMART GRIDS</b>  | <b>POWER QUALITY</b>  | <b>MODELLING &amp; SIMULATION</b>   | <b>RENEWABLE ENERGY</b>   |  |
| 1010-1030 | Chair: Dr Ramesh Rayudu<br><br>Novel WiMAX Usage Scenarios for Smart Grid Applications ( <i>Dr V. Sreeram - Uni of Western Australia</i> )  | Chair: Dr Vic Smith<br><br>Dc-link Capacitor Voltage Balancing for a Five-level Diode-clamped Active Power Filter Using Redundant Vectors ( <i>Dr H. Zhang; PRESENTER J. Yang - Uni of Strathclyde</i> )            | Chair: Dr Bill Heffernan<br><br>Sensitivity Analysis of Ferroresonance Simulations to Small Variations in Model Parameters and Initial Conditions ( <i>P. Moses - Curtin Uni</i> )                                | Chair: Prof Tapan Saha<br><br>Impact of Wind Turbine Penetration on the Dynamic Performance of Interconnected Power Systems ( <i>J. Hossain - UNSW@ADFA</i> )               |  |
| 1030-1050 | Home Area Network Technologies Assessment for Demand Response in Smart Grid Environment ( <i>Z. Huq - Curtin Uni</i> )  | Implementation of Closed Loop Voltage Control for Medium Voltage Distribution ( <i>J. Quinn - CQ Uni</i> )  | Impact of High Wind Generation Penetration on Frequency Control ( <i>Prof M. Negnevitsky - Uni of Tasmania</i> )  | Modelling of a Doubly Fed Induction Generator (DFIG) to Study its Control System ( <i>M. Billah - Swinburne Uni of Technology</i> )   |  |
| 1050-1120 | <b>MORNING TEA</b>  |   |   |   |  |
| 1120-1140 | <b>SMART GRIDS</b><br><br>Chair: Dr Ramesh Rayudu<br><br>Demand-Side Response Load Management Modelling Encountering Electrical Peak Demands in Eastern and Southern Australia - Smart Grid Tools ( <i>M. Marwan - Uni of Southern Queensland</i> ) | <b>POWER QUALITY</b><br><br>Chair: AscProf Sarah Perera<br><br>Damping of Large Turbo-Generator Subsynchronous Resonance using Superconducting Magnetic Energy Storage unit ( <i>Dr A. Abu-Siada - Curtin Uni</i> ) | <b>MODELLING &amp; SIMULATION</b><br><br>Chair: AscProf Richard Duke<br><br>Challenges of Economic Modelling for Transmission Investments ( <i>Dr N. Newham - Transpower NZ Ltd</i> )                             | <b>RENEWABLE ENERGY</b><br><br>Chair: Prof Pat Bodger<br><br>Fast Tracking Control for Maximum Output Power in Wind Turbine Systems ( <i>Prof D-C. Lee - Yeungnam Uni</i> ) |  |
| 1140-1200 | System Thevenin Impedance Estimation Through On-Load Tap Changer Action ( <i>M. Bahadorne; PRESENTER Dr N. Nair - Uni of Auckland</i> )   | Improving Voltage Quality with Series Active Filter Using Fuzzy Logic Control ( <i>Dr S.S. Mortazavi - Shahid Chamran Uni</i> )   | Reclosing Transients of Induction Motor with Terminal Capacitors during Source Interruption ( <i>Dr R. Hamouda - King Saud Uni</i> )  | AHP and fuzzy assessment based sustainability indicator for hybrid renewable energy system ( <i>Dr G. Liu - CQ Uni</i> )  |  |
| 1200-1220 | A Comprehensive Approach to Demand Response in Restructured Power Systems ( <i>T. Nguyen; PRESENTER Prof M. Negnevitsky - Uni of Tasmania</i> )   | The 230 V CBEMA Curve - Preliminary Studies ( <i>Dr V. Smith - Uni of Wollongong</i> )  | A novel winding structure in planar inductors to decrease the overall capacitive couplings ( <i>N. Shahabi Ghahfarokhi - Queensland Uni of Technology</i> )   | Achieving a Synergy by combining Air Conditioners and Photovoltaic Panels: an Evolutionary-Algorithm approach ( <i>C. Perfumo - CSIRO/Uni of Newcastle</i> )                |  |
| 1220-1320 | <b>LUNCH</b>  |   |   |   |  |
| 1320-1340 | <b>DISTRIBUTED GENERATION/ELECTRIC M&amp;D</b><br><br>Chair: Dr Wade Enright<br><br>Optimal Operation of DISCO in Restructured Power Market with Wind Farm and Interruptible loads Considerations ( <i>Dr S.S. Mortazavi - Shahid Chamran Uni</i> ) | <b>TRANSMISSION &amp; DISTRIBUTION</b><br><br>Chair: Dr Roger McKenzie<br><br>Impacts of HVAC Interconnection Parameters on Inter-area Oscillation ( <i>H.M. Nguyen - Uni of Queensland</i> )                       | <b>ELECTRIC MACHINES &amp; DRIVES</b><br><br>Chair: David Maples<br><br>Flux-switching Permanent Magnet Machine Drive System for Plug-in Hybrid Electrical Vehicle ( <i>Dr W. Xu - Uni of Technology Sydney</i> ) |   |  |
| 1340-1400 | Distributed generation systems for supplying residential electricity demand with considering emission penalties and total net present cost ( <i>A. Yousefi - Uni of Western Australia</i> )   | Voltage Unbalance Reduction in Low Voltage Distribution Networks with Rooftop PVs ( <i>F. Shahnia - Queensland Uni of Technology</i> )  | Electromagnetic Parameters of a Three Phase Transverse Flux Machine with an External Rotor for Wheel Hub Drives ( <i>Prof E. Schmidt - Vienna Uni of Technology</i> )   |   |  |
| 1400-1420 | Optimization of Distribution Transformer Using High Frequency Attained by SMPS Technology ( <i>Dr R. Khawaja - Rachna College of Engineering &amp; Technology</i> )   | A Thermal constraint Study of the Wellington Regional Transmission Network ( <i>Dr P. Paranavithana - Transpower NZ Ltd</i> )   | ANN-Based Flux Observer for the Sensor-Less Control of a Permanent Magnet Synchronous Motor ( <i>Dr M. Saqib - Uni of Engineering &amp; Technology, PAK</i> )   |   |  |
| 1420-1520 | <b>AUPEC 2010 CLOSING</b><br><b>PRESENTATIONS &amp; AWARDS</b>  |   |   |   |  |
|           | Chair: AscProf Richard Duke & Co-Chair: Prof Pat Bodger   |   |   |   |  |